

*Third International Symposium on the Effects of Surface Geology on Seismic Motion
Grenoble, France, 30 August - 1 September 2006
Paper Number: xxx*

One- and Two-Dimensional Benchmark Results from Pacific Engineering and Analysis

Bob Darragh, Walt Silva, and Nick Gregor

Pacific Engineering and Analysis, El Cerrito, California, United States of America (USA)

ABSTRACT –A finite-source stochastic one-dimensional ground motion model, coupled to vertically propagating equivalent-linear shear-wave site response models was used to estimate the ground motions for the one- and two-dimensional benchmarks. This model has been validated for nineteen well-recorded earthquakes, **M** 5.6 to 7.6 at over 600 sites.

Median peak accelerations ranging from 0.115 g (at station R01) to 0.218 g (at station R09) are estimated at the nine surface sites for the two-dimensional benchmark (S1 **M**6) from a non-linear analysis incorporating EPRI modulus-reduction and damping curves and parametric uncertainty. Median values of peak acceleration, velocity and displacement along with the 16th to 84th percentile ranges in parenthesis at R05 are 0.14 g (0.109 to 0.184 g), 20.3 cm/sec (14.7 to 28.0 cm/sec) and 8.9 cm (5.3 to 15.2 cm). Corresponding values from the linear analysis are 0.22 g (0.165 to 0.293 g), 21.1 cm/sec (15.5 to 28.7 cm/sec) and 8.7 cm (5.1 to 14.8 cm).

Median values of peak acceleration, velocity and displacement along with the 16th to 84th percentile ranges in parenthesis at R10 (at depth) are 0.072 g (0.057 to 0.090 g), 6.4 cm/sec (5.1 to 8.0 cm/sec) and 3.4 cm (2.5 to 4.7 cm).

Median values of peak acceleration along with the 16th to 84th percentile ranges in parenthesis at R05 and R10 for the **M** 2.9 (W1) are 0.0124 g (0.0098 to 0.0156 g) and 0.0046 g (0.0041 to 0.0052 g), respectively.

Source Models

The finite- and point-source models used here are stochastic (Boore, 1983; Silva, 1992; Schneider et al., 1993) and use simple plane wave geometrical attenuation. The point-source model uses $1/R$ ($1/\text{SQRT}(R)$), $R > 2$ crustal thicknesses) modified for magnitude dependencies (Silva et al., 1997) while the finite-source model uses ray tracing (Ou and Hermann, 1990) from each subfault to the site. Both models have been validated with nineteen earthquakes at over 600 sites (Silva et al., 1997; BSC 2004; Darragh et al., 2006).

Site response method

For these analyses the conventional one-dimensional (1D) approach to estimating the effects of site-specific site conditions on strong ground motions that assumes vertically propagating plane shear-waves for the horizontal components is used. Input and output motions may be either outcrop or total (within layer) motions and the solution scheme (Silva, 1976; Johnson and Silva, 1981) is exact for a layered system.

Dynamic material nonlinearities are accommodated through the equivalent-linear approximation that employs a random vibration theory (RVT) approach to estimate strain levels (EPRI, 1993). Random process theory is used to predict peak time domain values of shear-strain based upon the shear-strain power spectrum. The purely frequency

domain approach obviates a time domain control motion and, eliminates the need for a suite of analyses based on different input motions. This arises because each time domain analysis may be viewed as one realization of a random process. In the case of the frequency domain approach, the estimates of peak shear-strain as well as oscillator response are, as a result of the random process theory, fundamentally probabilistic in nature. For fixed material properties, stable estimates of site response can then be obtained with a single run.

While the assumptions of vertically propagating shear waves and equivalent-linear soil response certainly represent approximations to actual conditions, their combination has achieved demonstrated success in modeling the effects of site conditions on strong ground motions, particularly 5% damped response spectra. (Schnabel et al., 1972; Silva et al., 1988; Schneider et al., 1993; EPRI, 1993; BSC, 2004). At high loading levels and for soft soils, the equivalent-linear approximation, because it typically uses frequency independent damping, as well as, shear-wave velocities, will overdamp high frequencies compared to fully nonlinear analyses. However, for design purposes, it is the 5% damped response spectra which is important and, because of its natural smoothing effects at high frequency, response spectra computed with equivalent-linear analyses compare very favorably with recorded data as well as with fully nonlinear analyses (EPRI, 1993; Silva et al., 2000, BSC, 2004).

Incorporation of site parameter variability

Since seismic hazard for engineering design is typically defined as a rock (firm site condition) outcrop UHS (Uniform Hazard Spectrum), or a fractile level (5% damped response spectra) for deterministic definitions, corresponding soil design spectra must preserve the annual probability of exceedence of the rock UHS or fractile level of the deterministic criterion. This requirement, essential for performance based design, necessitates an approach to site response that properly accommodates, in a statistically significant manner, aleatory variability (randomness) in site-specific dynamic material properties. To achieve this goal, a methodology has been developed which employs randomly generated shear-wave velocity profiles as well as G/G_{max} and hysteretic damping curves (EPRI, 1993; Silva et al., 1997; McGuire et al., 2001). Corresponding site response analyses and response spectra are computed for each realization producing estimates of median and $\pm 1 \sigma$ values. The range of median to $\pm 1 \sigma$ then represents the effect of aleatory parametric variability on expected motions. This parametric variability is intended to reflect spatial variability as well as both aleatory and epistemic (uncertainty) measurement variability.

The measurement variability is taken to reflect the combined effects of variability about mean properties (aleatory) as well as variability of mean properties (epistemic). For G/G_{max} and hysteretic damping curves, epistemic variability arises when different values are obtained from the same material sample but using different test devices (e.g. resonant column, torsional shear, cyclic triaxial). Additionally epistemic variability arises from the same device with varying confining pressures, near the estimated in-situ value, since the true in-situ confining pressure is generally unknown. As well as these effects, sample disturbance can significantly alter a soil's dynamic material properties, resulting in an uncertainty in the best estimate or mean value for both the modulus reduction and hysteretic damping curves.

For shear-wave velocity, measurement epistemic variability may be due to a range in base case shear-wave velocity profiles resulting from different measurement techniques (e.g. downhole, crosshole, suspension, SASW) at the same site location. Additionally, measurement epistemic variability in shear-wave velocity can arise when the

measurement is not taken at the site (point) of interest, but nearby, generally meters to hundreds of meters away. This is especially the case for SASW, which has a linear array that typically spans a surface length at least twice the depth of velocity estimate. These epistemic variabilities are difficult to estimate and require clusters of measurements using all four approaches at sites with varying conditions: hard, stiff, firm, and soft (deep). As a result, we generally make the assumption that this epistemic variability is accommodated in the parametric aleatory variability either intrinsically or as a neglected small contributor: recall with variabilities it is the variances that add, not the standard deviations. As such, for example, a parametric variability of 0.40 ($\ln \sigma$) and an epistemic variability of 0.20 results in a total variability of 0.45, neglecting covariances (which is generally done).

Spatial variability, for typical design cases, reflects lateral variability over the footprint of a structure. This is generally considered aleatory variability. For G/G_{max} and hysteretic damping curves, laboratory dynamic testing (with a single device) shows a range in values for samples taken of the same material type and depth range. If a particular material type and sample depth range reflects conditions that would imply use of a single set of curves (mean values) to predict future motions, this variability is parametric aleatory and must be properly accommodated through randomization in developing design motions (to preserve realistic estimates of mean motions and fractiles). If, on the other hand, sample disturbance was judged to be significant, for example, judgment is sometimes used to compensate for any potential effects (EPRI, 1993). Such judgment typically results in multiple estimates or corrections, resulting in multiple sets of curves for each depth range. This variability is epistemic and must be treated quite differently in estimating design motions, generally by developing multiple estimates of motions or hazard curves and applying weights, to preserve the probability levels of the fracture estimate.

To accommodate these parametric variabilities in design motions, shear-wave velocity profiles as well as G/G_{max} and hysteretic damping curves are randomized about best estimate or base case values. As previously discussed, the motivation for developing the randomization or probabilistic methodology was in applications to typical design cases where site specific soil design spectra are desired, typically conditional on a rock outcrop UHS or deterministic spectra, and which accommodate local or site wide (footprint) variability. For an application such as the Grenoble benchmarks, where site or footprint dimensions are small, the assumption is that motion at a point, due to lateral heterogeneity, is influenced by dynamic material properties at horizontal distances beyond the point. In other words, the multiple 1D analysis with randomized properties are assumed to accommodate 2D effects due to random lateral heterogeneity. With this assumption we have used our typical empirical distribution intended to approximately capture random horizontal spatial variability through multiple 1D analyses. Deterministic 2D and 3D effects may approximately be accommodated with alternate 1D columns through the 2D or 3D structure or simply a single 1D structure with sufficient soil thickness (Hartzell et al., 2004)

The profile randomization scheme, which varies both layer velocity and thickness as well as depth to "rock" (soil depth), is based on a correlation model developed from an analysis of variance on about 500 measured shear-wave velocity profiles (EPRI, 1993; Silva et al., 1997). In general the algorithm accommodates depth dependent empirical distributions of shear-wave velocity at each depth in addition to a vertical correlation of velocity with depth. Velocity fluctuations between layers is then conditional on the depth dependent correlations. The scheme is intended to capture realistic lateral variations in shear-wave velocity due to natural heterogeneity.

To accommodate variability in the modulus reduction and damping curves on a generic basis, the curves are independently randomized about the base case values. A log

normal distribution is assumed with a σ_{in} of 0.30 at a cyclic shear strain of $3 \times 10^{-2}\%$ with upper and lower bounds of 2σ . The distribution is based on an analysis of variance of measured G/G_{max} and hysteretic damping curves and is considered appropriate for applications to generic (material type specific) nonlinear properties. The truncation is necessary to prevent modulus reduction or damping models that are not physically possible. The random curves are generated by sampling the transformed normal distribution with a σ_{in} of 0.30, computing the change in normalized modulus reduction or percent damping at $3 \times 10^{-2}\%$ shear strain, and applying this factor at all strains. The random perturbation factor is reduced or tapered near the ends of the strain range to preserve the general shape of the median curves (Silva, 1992).

For each site location (R01 to R10), thirty realizations are performed to capture stable estimates of the median and reasonably stable estimates of the standard deviation in motions (5% damped response). Thirty realizations are sufficient for stable estimates of the median (\leq about 5%) but results in about a 30% variation in the estimate of the standard deviation. About three hundred realizations are necessary to obtain less than about a 5% variation (accuracy) in the standard deviation (McGuire et al, 2001). Since the major interest in this benchmark study are median estimates, a 30% uncertainty (epistemic) in the aleatory variability is considered acceptable.

Incorporation of model variability

In addition to the parametric variability, model variability should be accommodated in expected motions. Model variability, an expression of how well the model works, or model error, is generally estimated by comparing computed motions to recorded motions through validation exercises. It is typically estimated as a Chi-Square between 5% damped response spectra computed from recorded motions and spectra estimated from analyses (EPRI 1993; Silva et al., 1997). For stable estimates of model variability, at least twenty samples (recordings) are required which, for applications to site response analyses, requires vertical arrays, which have known input and output motions, and which must have known and reliable dynamic material properties. Additionally, multiple arrays should be used, sampling a wide range in site conditions as well as varying loading levels. We have initially evaluated model variability using data recorded at seven vertical arrays. Because there are not sufficient data to smooth the frequency-to-frequency variability, a value of 0.35 (σ_{in}) is assumed which is independent of frequency and appropriate for both surface and at-depth analyses (Darragh and Silva, 2006).

Estimates of model parameters

The 5% damped response spectral ratio (R05/R10) of the acceleration data (differentiated from the recorded velocity time history) from the 2003/04/26, $M_I=2.9$ Lancey event recorded by the French accelerometric network is shown as the solid line in Figure 1. This event is Weak Case #1 and was recorded at OGFH (R05: surface station at top of borehole) and OGFB (downhole). OGFB (R10) is located at 535 m depth and corresponds to that of receiver#10 (R10) of the 2D benchmark. The response spectral ratio (R05/R10) estimated from the linear-elastic response of the shear-wave velocity and density profile provided for the benchmark (i.e. V_s (m/sec) = $(300 + 19 \sqrt{D})$; density (gm/cc) = $(2140 + 0.125 D) / 1000$ with bedrock at 541.5 m) is shown as the dashed line. At short period (high frequency) the recorded data show larger amplification (close to 5) than the model (close to 4), which suggests lower shear-wave velocity material in the top 12 m approximately. Hence the shear-wave model provided may lead to an under prediction of the motion at the surface.

Point source analyses were also performed to estimate kappa (Anderson and Hough, 1984). Figures 2 and 3 show the 5% damped response spectra for the Lancey event compared to the 16th, median and 84th percentiles from a stochastic one-dimensional model at depth (R10) and the surface (R05). A kappa of 0.025 sec fits the recorded data, in terms of response spectral shape, satisfactorily and this value is used in the benchmark analyses.

Results: 1D and 2D benchmarks

We estimated the variability in the acceleration, velocity and displacement time histories for the 1D benchmark: (M 6.0 Free-Style Prediction at stations R05 (OGFH, borehole at the surface)) and 2D benchmarks: S1 (**M6.0**) and W1 (**M2.9**) at stations R01 to R10: in the following manner. Two sets of modulus-reduction and damping curves were used; EPRI and Peninsular Range (PR) (EPRI, 1993). The use of two different sets of curves reflects the epistemic variability in these soil parameters at this site. For each case (EPRI or PR curves) we computed 30 different realizations randomly varying the shear-wave velocity structure, soil modulus-reduction and damping parameters, stress drop, crustal Q, kappa, as well as, the slip distribution and rupture nucleation point in our finite fault simulation. This is parametric aleatory or variability.

Figure 4 shows the median, 16th and 84th percentiles 5% damped response spectra for R05 using EPRI curves computed for both the 1D and 2D benchmarks. The median peak acceleration, velocity and displacement are 0.143 g, 20.3 cm/sec and 8.9 cm. Using PR modulus-reduction and damping curves the median peak values are 0.134 g, 13.7 cm/sec and 8.8 cm. Only parametric uncertainty or variability is included in the 16th and 84th percentile spectra shown on this figure. Model variability, if included in the calculation of these percentiles, would significantly increase the range due to the addition of a factor of 0.35 (σ_{ln}).

In addition, for each set of modulus-reduction and damping curves (EPRI or PR) linear estimates were also made for the same 30 realizations to provide an estimation of the importance of non-linear effects. Figure 5 shows the linear 5% damped response spectra at R05 using EPRI curves. The peak acceleration is 0.220 g, a significant increase of more than 50%. In addition, the peak response has shifted to lower periods (higher frequencies) as expected. The long period response (> 1 sec) is quite similar for both the non-linear (Figure 4) and linear calculations (Figure 5) at this site. Median values of peak acceleration, velocity and displacement along with the 16th to 84th percentile ranges in parenthesis from the linear analysis are 0.220 g (0.165 to 0.293 g), 21.1 cm/sec (15.5 to 28.7 cm/sec) and 8.7 cm (5.1 to 14.8 cm).

Figure 6 is an example of the acceleration, velocity and displacement time histories computed for an average horizontal component at R05 for the base case profile (no randomization). The waveforms appear reasonable in amplitude and phasing for a **M6** earthquake at about 8 km distance.

Figures 7 and 8 show the median, 16th and 84th percentiles 5% damped response spectra for all ten stations in the 2D benchmarks S1 and W1, respectively. These figures show the variability in response across the surface array of stations (R01 to R09) and at depth (R10). The spectra for the **M2.9** earthquake are narrow-band with a peak generally near 20 to 25 Hz. The peak accelerations at 0.01 sec (100 Hz) are also about a factor of 10 smaller than for the **M6**. In both cases, the motion at depth (R10) is smaller than at the surface at short periods.

References

- Anderson, J. G. and S. E. Hough (1984). A model for the shape of the Fourier amplitude spectrum of acceleration at high frequencies. *Bulletin of the Seismological Society of America*, 74(5), 1969-1993.
- Boore, D.M. (1983). Stochastic simulation of high-frequency ground motions based on seismological models of the radiated spectra. *Bulletin of the Seismological Society of America*, 73(6), 1865-1894.
- BSC (Bechtel SAIC Company) (2004). Development of earthquake ground motion input for preclosure seismic design and postclosure performance assessment of a geologic repository at Yucca Mountain, NV, MDL-MGR-GS-000003 REV 1. Las Vegas, Nevada: Bechtel SAIC Company.
- Darragh, R. B. and W. J. Silva (2006). Turkey Flan – Blind Prediction: Phase 2 Submitted to California Geological Survey.
- Darragh, R., W. Silva and Gregor, N. (2006). Validation and comparison of one-dimensional ground motion methodologies, ESG 2006: Third International Symposium on the Effects of Surface Geology on Seismic Motion, Grenoble, France, 885-895.
- Electric Power Research Institute (1993). Guidelines for determining design basis ground motions. Palo Alto, California: Electric Power Research Institute, vol. 1-5, EPRI TR-102293.
- Hartzell, S., L. F. Bonilla and R. A. Williams (2004). Prediction of nonlinear soil effects. *Bulletin of the Seismological Society of America*, 94(5), 1609-1629.
- Johnson, L.R., and Silva, W. (1981). The effects of unconsolidated sediments upon the ground motion during local earthquakes. *Bulletin of the Seismological Society of America*, 71(1), 127-142.
- McGuire, R.K., W.J. Silva and C.J. Costantino (2001). Technical basis for revision of regulatory guidance on design ground motions: hazard- and risk-consistent ground motions spectra guidelines. Prepared for Division of Engineering Technology, Washington, DC, NUREG/CR-6728.
- Ou, G.B. and R. B. Herrmann (1990). Estimation theory for strong ground motion. *Seismological Research Letters*. 61.
- Schnabel, P.B., Lysmer, J., and Seed, H.B. (1972). SHAKE: a computer program for earthquake response analysis of horizontally layered sites. Earthquake Engineering Research Center, University of California at Berkeley, EERC 72-12.
- Schneider, J.F., W.J. Silva, and C.L. Stark (1993). Ground motion model for the 1989 M 6.9 Loma Prieta earthquake including effects of source, path and site. *Earthquake Spectra*, 9(2), 251-287.
- Silva, W.J. (1976). Body waves in a layered anelastic solid. *Bulletin of the Seismological Society of America*, 66(5), 1539-1554.
- Silva, W.J. (1992). Factors controlling strong ground motions and their associated uncertainties. *Dynamic Analysis and Design Considerations for High Level Nuclear Waste Repositories*, ASCE 132-161.
- Silva, W. J.; Turcotte, T.; Moriwaki, Y. (1988). Soil Response to Earthquake Ground Motion. Electric Power Research Institute, Walnut Creek, California, Report No. NP-5747.
- Silva, W.J., N. Abrahamson, G. Toro and C. Costantino (1997). Description and validation of the stochastic ground motion model. Report Submitted to Brookhaven National Laboratory, Associated Universities, Inc. Upton, New York 11973, Contract No. 770573.
- Silva, W.J., R. Darragh, N. Gregor, G. Martin, C. Kircher, N. Abrahamson (2000). A Reassessment of site coefficients and near-fault factors for building code provisions. @ Final Report USGS Grant award #98-HQ-GR-1010.

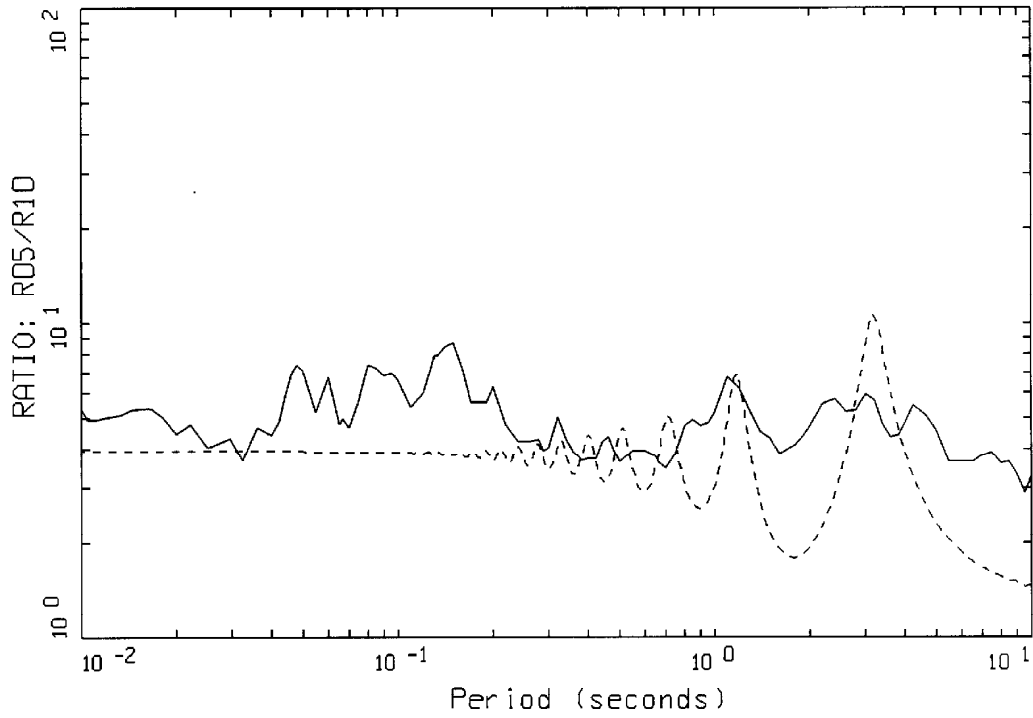


FIGURE 1 - 5% DAMPED SPECTRAL RATIO
SURFACE/DEPTH, AVERAGE HORIZONTAL

LEGEND
—— LANCEY EARTHQUAKE: 2003/04/26 ML=2.9
----- RASCALS: LINEAR ELASTIC CASE

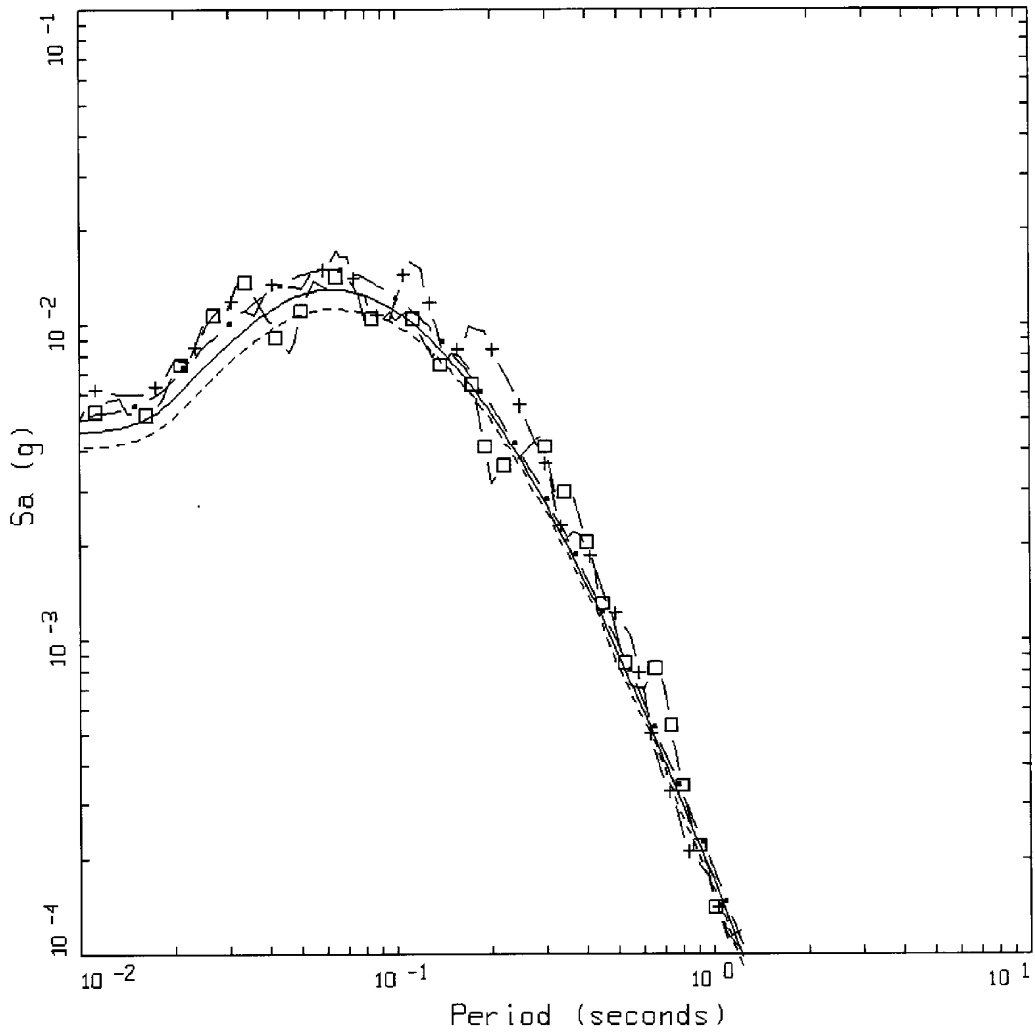


FIGURE 2 - R10 (AT DEPTH), EPRI CURVES
 M = 3.2, D = 7.57 KM, H=3.0 KM, KAPPA=0.025 SEC

LEGEND

- • — 84TH PERCENTILE, PARAMETRIC UNCERTAINTY; PGA = 0.0052 G
- 50TH PERCENTILE, PARAMETRIC UNCERTAINTY; PGA = 0.0046 G
- 16TH PERCENTILE, PARAMETRIC UNCERTAINTY; PGA = 0.0041 G
- + — 5 %, EAST, LANCEY EARTHQUAKE
- □ — 5 %, NORTH, LANCEY EARTHQUAKE

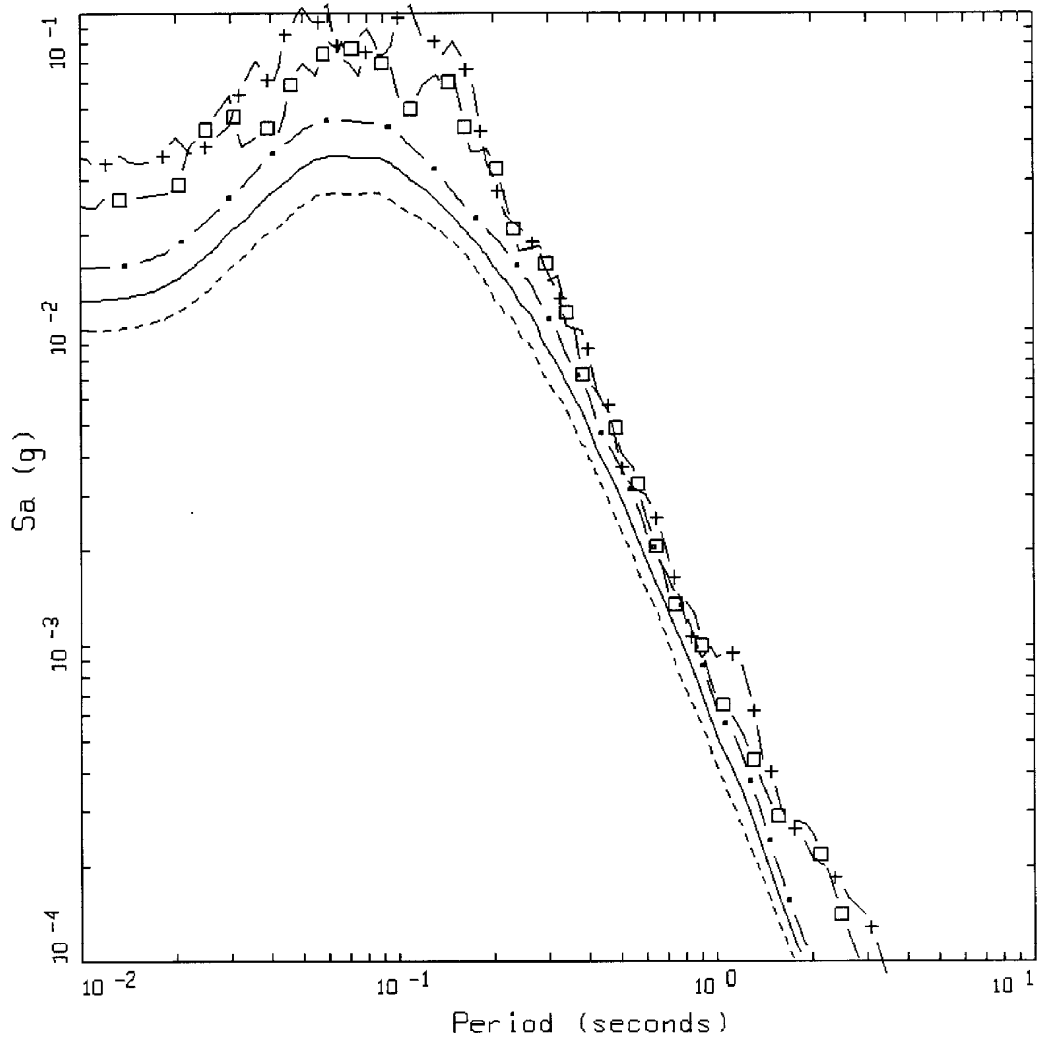


FIGURE 3 - R05 (SURFACE), EPRI CURVES
 $M = 3.2$, $D = 7.57$ KM, $H = 3.0$ KM, $KAPPA = 0.025$ SEC

- LEGEND
- . - 84TH PERCENTILE, PARAMETRIC UNCERTAINTY; PGA = 0.0129 G
 - 50TH PERCENTILE, PARAMETRIC UNCERTAINTY; PGA = 0.0103 G
 - - - - 16TH PERCENTILE, PARAMETRIC UNCERTAINTY; PGA = 0.0082 G
 - + - 5 %, EAST, LANCEY EARTHQUAKE
 - □ - 5 %, NORTH, LANCEY EARTHQUAKE

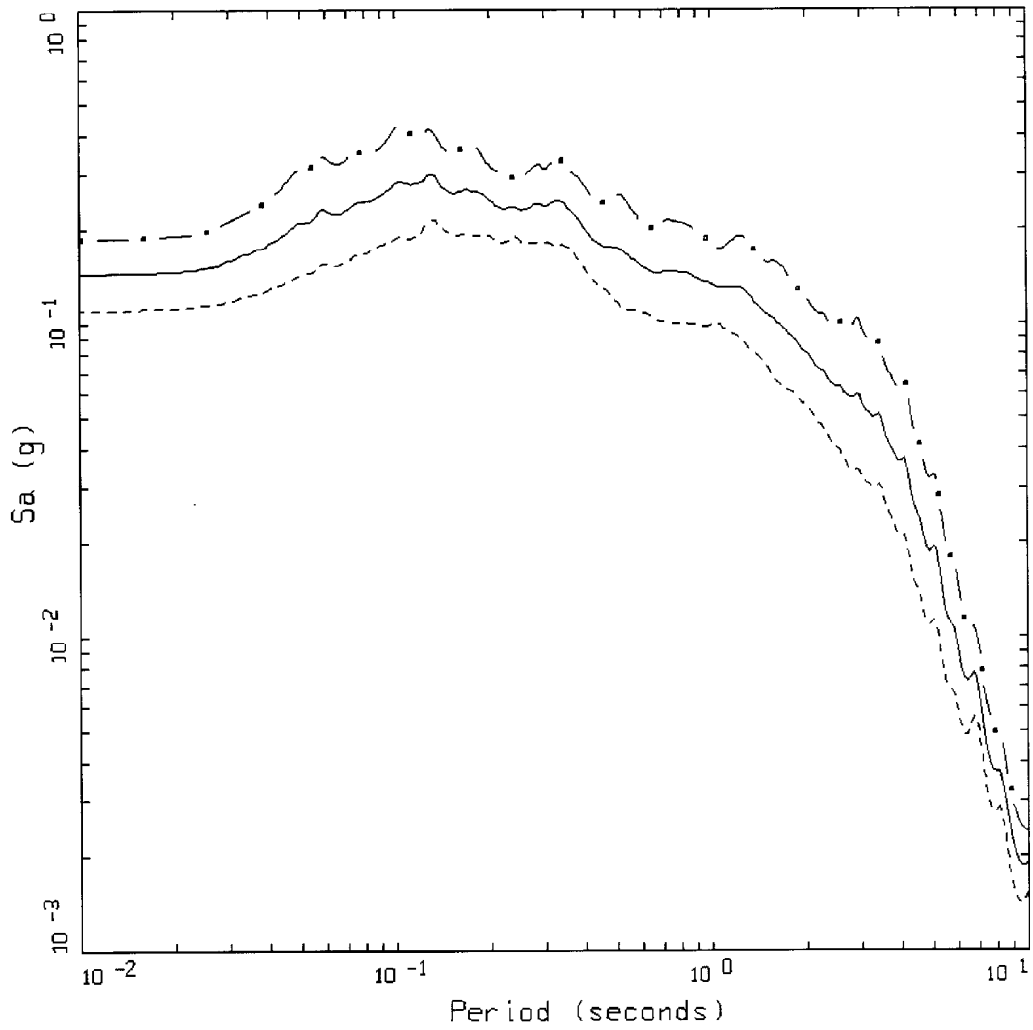


FIGURE 4 - R05
M = 6.0, EPRI CURVES, NONLINEAR

- LEGEND
- • — 84TH PERCENTILE, PARAMETRIC UNCERTAINTY; PGA = 0.185 G
 - — — 50TH PERCENTILE, PARAMETRIC UNCERTAINTY; PGA = 0.143 G
 - 16TH PERCENTILE, PARAMETRIC UNCERTAINTY; PGA = 0.111 G

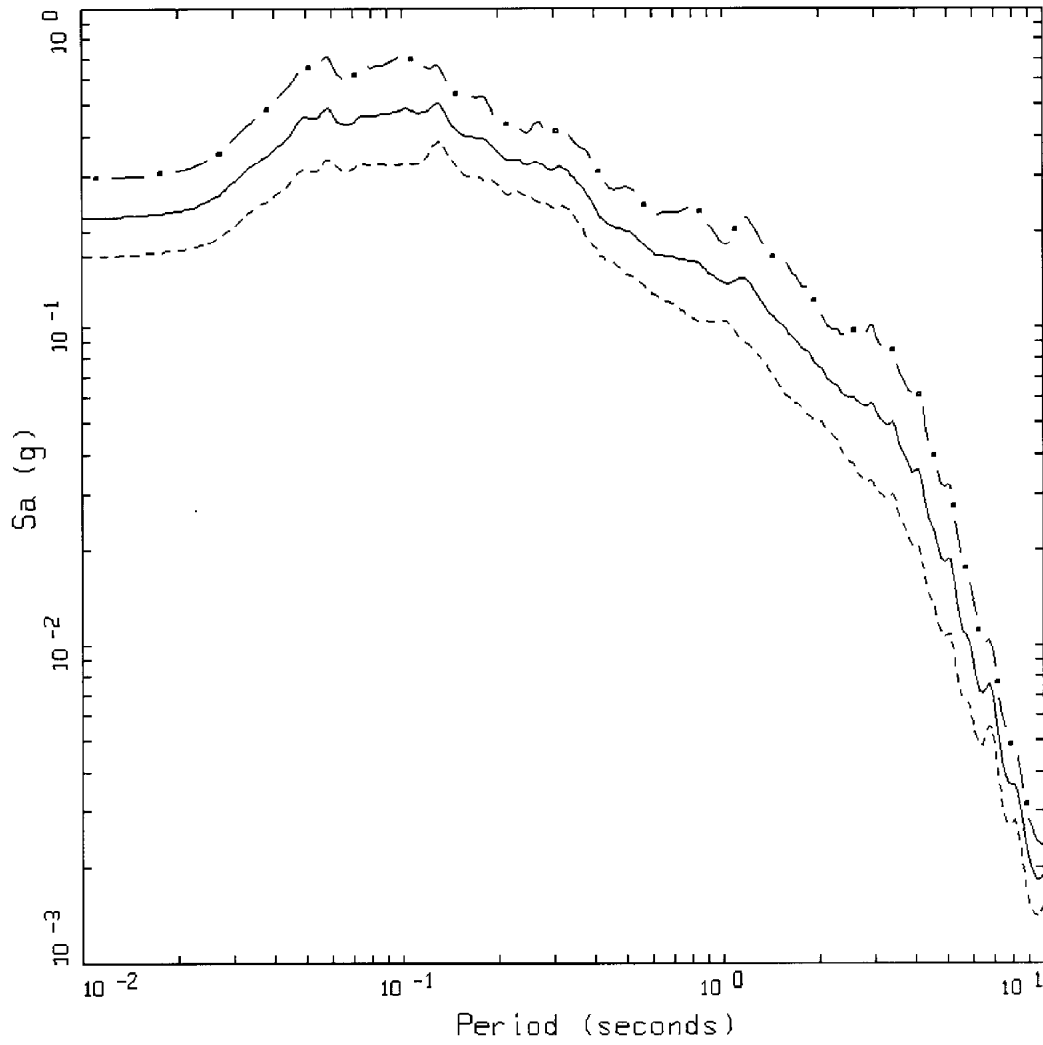


FIGURE 5 - RD5
M = 6.0, EPRI CURVES, LINEAR

- LEGEND
- . - 84TH PERCENTILE, PARAMETRIC UNCERTAINTY; PGA = 0.100 G
 - 50TH PERCENTILE, PARAMETRIC UNCERTAINTY; PGA = 0.087 G
 - - - 16TH PERCENTILE, PARAMETRIC UNCERTAINTY; PGA = 0.075 G

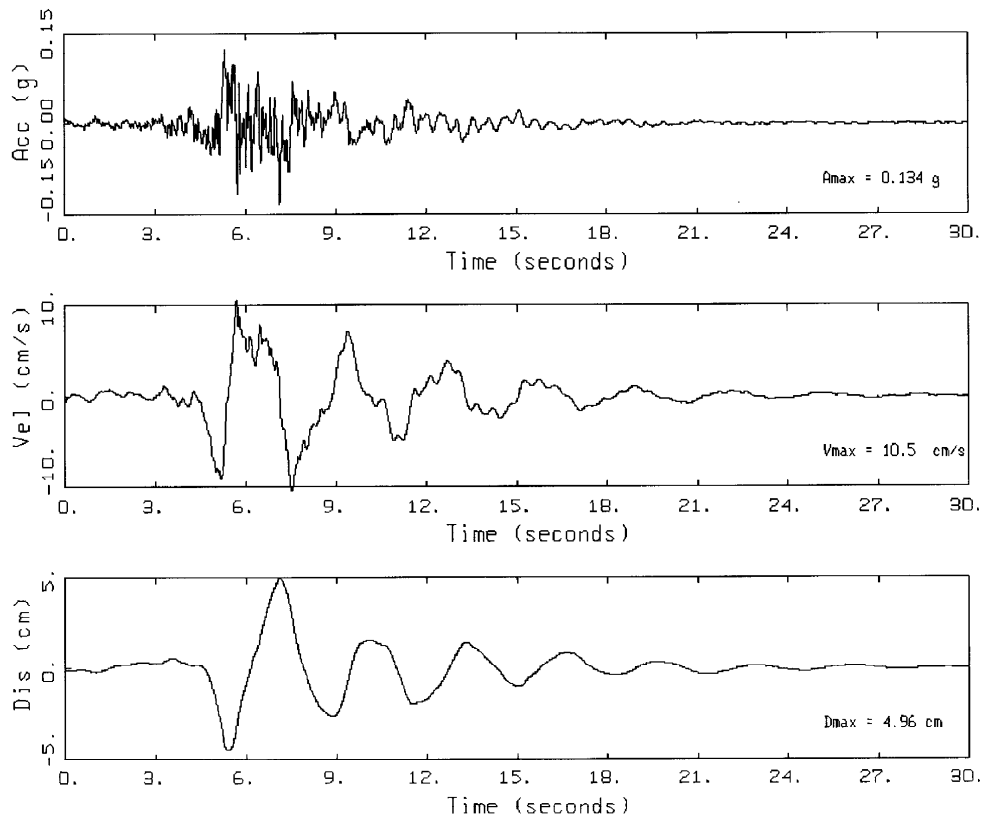


FIGURE 6 - R05: M=6.D, EPRI CURVES, BASE CASE

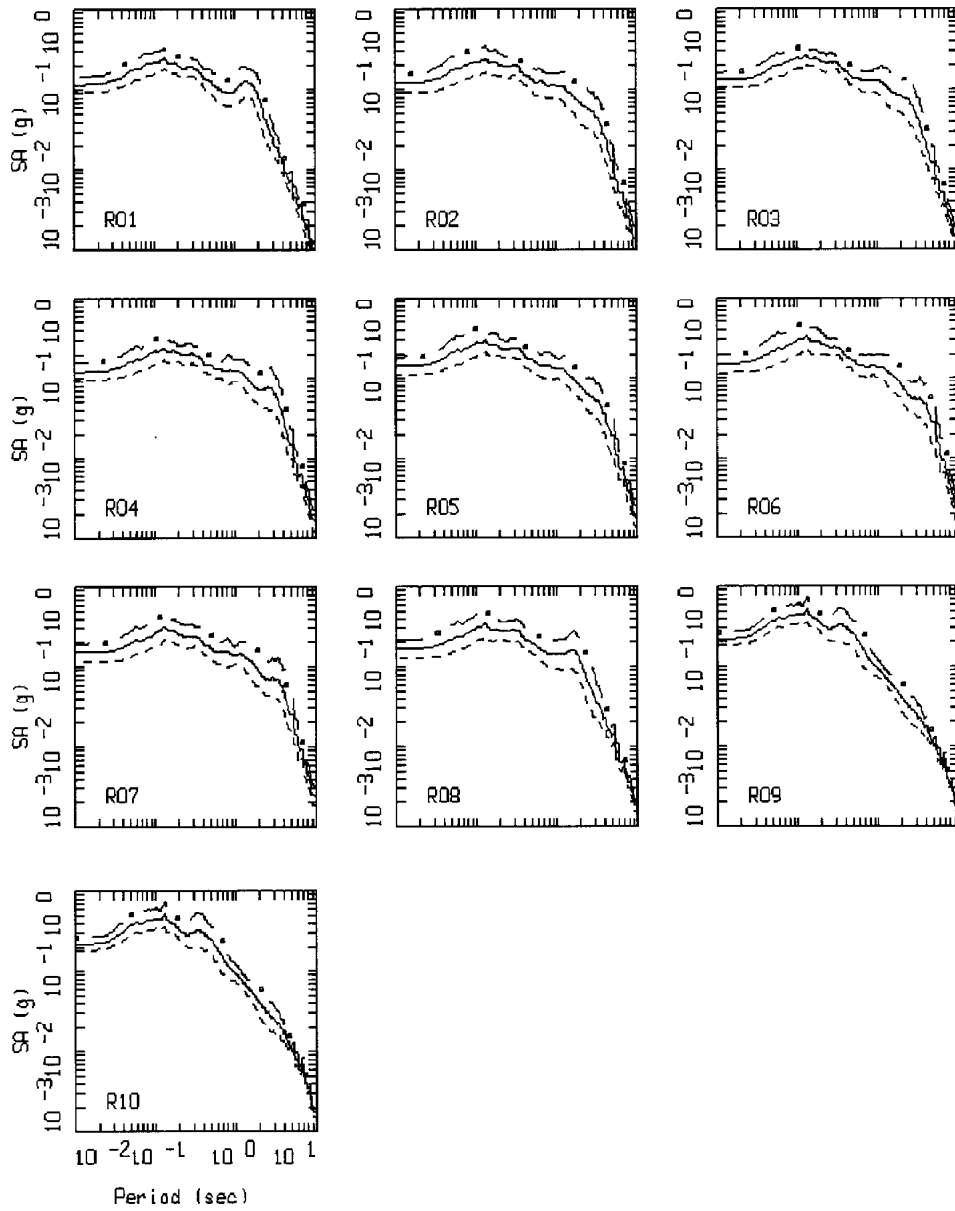


FIGURE 7 - 2D BENCHMARK S1: M 6.0
FINITE SOURCE MODELING: EPRI CURVES, NONLINEAR

LEGEND
 - . - 84TH PERCENTILE
 - - - 50TH PERCENTILE
 - - - 16TH PERCENTILE

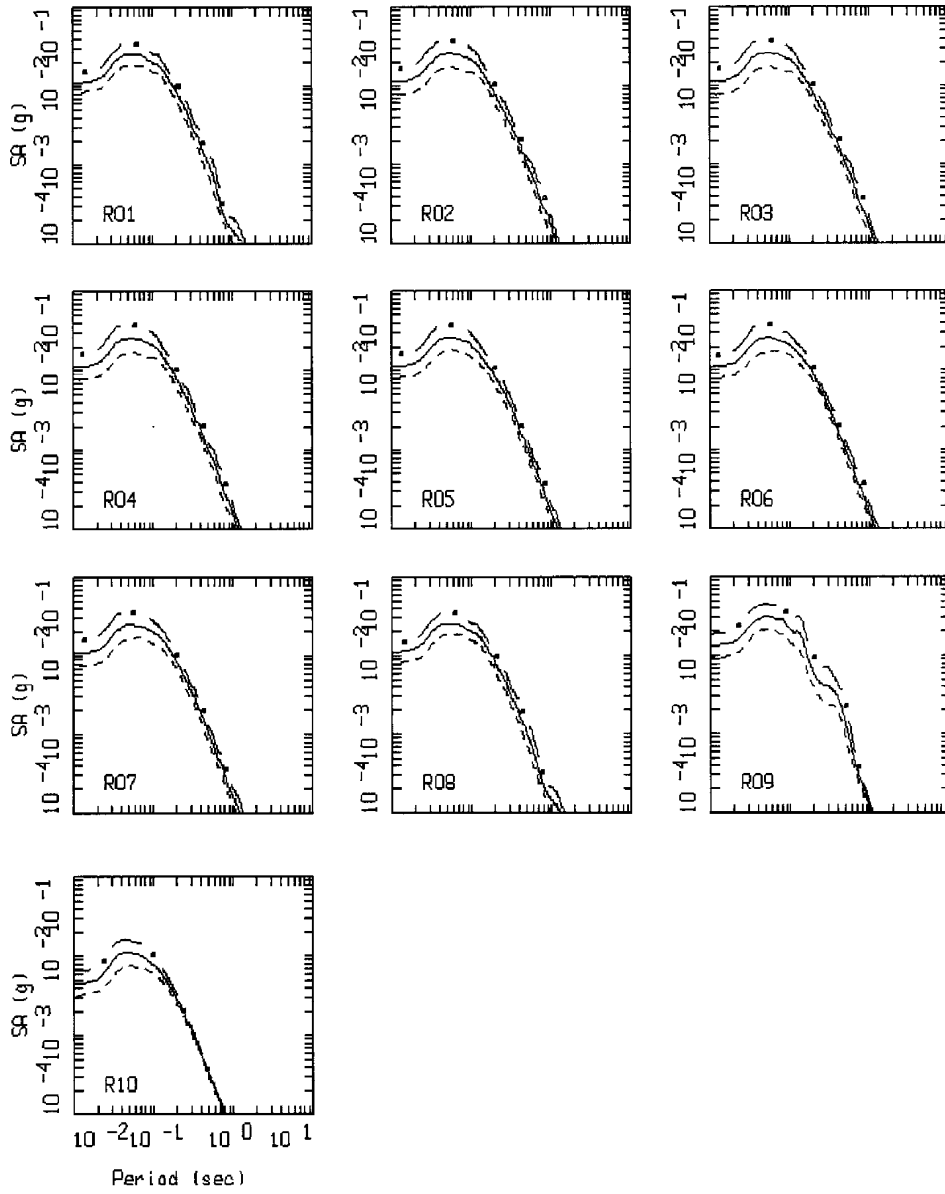


FIGURE 8 - 2D BENCHMARK W1; M 2.9
 POINT SOURCE MODELING: EPRI CURVES, NONLINEAR

LEGEND
 - . - 84TH PERCENTILE
 ——— 50TH PERCENTILE
 - - - - 16TH PERCENTILE